ELSEVIER

Journal of Hazardous Materials 85 (2001) 53–72

Journal of Hazardous Materials

www.elsevier.com/locate/jhazmat

Determination of the environmental impact of consolidation induced convective transport through capped sediment

Horace Moo-Young [a,*], Tommy Myers [b], Barbara Tardy [b], Richard Ledbetter [b], Wipawi Vanadit-Ellis [b], Kassahun Sellasie [a]

[a] *Department of Civil and Environmental Engineering, Lehigh University, Bethlehem, PA 18015-3188, USA*
[b] *Waterways Experiment Station, Vicksburg, MS, USA*

Abstract

The presence of contaminated sediment poses a barrier to essential waterway maintenance and construction in many ports and harbors, which support 95% of US foreign trade. Cost effective solutions to remediate contaminated sediments in waterways need to be applied. Capping is the least expensive remediation alternative available for marine sediments that is unsuitable for open water disposal. Dredged material capping and in situ capping alternatives, however, are not widely used because regulatory agencies are concerned about the potential for contaminant migration through the caps.

Numerous studies have been conducted on the effects of diffusion through caps, however, there is a lack of experimental data documenting the effects of consolidation induced transport of contaminants through caps. This study examines consolidation induced convective contaminant transport in capped sediment utilizing a research centrifuge. In this study, consolidation induced convective transport was modeled for 7 h at 100 × *g*, which modeled a contaminant migration time of 8 years for a prototype that was 100 times larger than the centrifuge model. In this study, hydrodynamic dispersion was a function of the seepage velocity. And, advection and dispersion dominated the migration of contaminants. Centrifuge model results were compared to an analytical solution for advection and dispersion. The advection–dispersion equation demonstrated that the centrifuge test is a conservative estimate for predicting contaminant transport. In conducting sensitivity analysis of the advection–dispersion equation to the centrifuge modeling, as hydrodynamic dispersion decreased, the time for contaminant breakthrough increased. Moreover, as the sediment to water distribution coefficient increased, the contaminant concentration into the overlying water decreased.

Keywords: Sediment; Capping; Research centrifuge; Environmental impact; Consolidation

*Corresponding author. Tel.: +1-610-758-6851; fax: +1-610-758-6851.
E-mail address: hkm3@lehigh.edu (H. Moo-Young).

0304-3894/01/$ – see front matter
PII: S0304-3894(01)00221-7

1. Introduction

Approximately 523 million cubic meters of sediment must be dredged from waterways and ports each year to maintain the nation's navigation system (with approximately 18–37 million cubic meters of contaminated sediment). The presence of contaminants in the sediment has changed the state of practice in the dredging industry (National Research Council, NRC [1]). Economics, technical feasibility, and environmental acceptability must be evaluated to determine the most appropriate option. There are three alternatives for the disposal of marine sediment: open water disposal (e.g. sub-aqueous pits), confined disposal facilities, and beneficial use applications. Of the approximately 523 m^3 of marine sediment, 444 m^3 are placed in inland, coastal, and estuarine open water sites, confined disposal facilities, or beneficial use sites [2–5].

When materials are unsuitable for ocean disposal, there are four basic options for remediation of contaminated sediment: containment in-place, treatment in-place, removal and containment, and removal and treatment. Economic considerations make decontamination and upland disposal options unfavorable to many port authorities [5]. In situ capping of sediment and disposal of contaminated sediments in sub-aqueous pits are the least expensive alternative. In situ capping involves placing a cap over contaminated sediment (i.e. in situ). In general, an in situ cap serves three purposes: to isolate contaminated material from the benthic environment, stabilize the contaminated material and reduce the potential for resuspension, and reduce the flux of dissolved contaminants into the overlying water. Previous studies have shown that both fine and course grained material can be utilized as the cap. For economic reasons, capping material is usually taken from areas that also require dredging. Palermo et al. [4] describe the best management practices for in situ capping of contaminated sediment. In sub-aqueous pit disposal, contaminated marine sediment is capped with a layer of clean sand, thus reducing the environmental impact of the sediment from the surrounding ecosystem. Environmental regulations have limited the use of in situ sediment capping due to the concerns about the contaminant migration through the cap [1].

Laboratory procedures are available for estimating contaminant migration from sediment into caps by diffusion [4,6–8], but diffusion is only one of the processes that affect capping effectiveness. Movement of contaminated pore water from sediment into caps due to sediment consolidation during and after cap placement may be much more significant than contaminant diffusion into caps. There is a basic lack of information on the significance of consolidation induced convective (advective) transport of contaminants from contaminated sediment into caps. Estimating the amount of convective contaminant transport due to consolidation is usually not performed when designing a capping layer [4]. The objective of this research is to evaluate the significance of consolidation induced convective transport of radiolabeled inorganic contaminants from sediment into caps using a research centrifuge. To accomplish this objective, the following tasks were conducted:

1. Cap and sediment soils were chemically and physically characterized.
2. Batch equilibrium tests were conducted to determine the adsorption potential of the capping material.
3. A centrifuge consolidation test was conducted to measure the settlement of the sediment and cap.

Table 1
Centrifuge scaling relationships

Quantity	Prototype	Model
Length	N	1
Area	N^2	1
Volume	N^3	1
Velocity	1	N
Acceleration	1	N
Mass	N^3	1
Force	N^2	1
Stress	1	1
Strain	1	1
Time (advection)	N^2	1

4. A centrifuge test was conducted to evaluate the significance of consolidation induced convective transport of radiolabeled inorganic contaminants through caps.
5. The centrifuge test result was compared to the predictions made using the advection–dispersion equation.

2. Literature review on centrifuge research

A typical laboratory column model of the sediment-cap prototype is not capable of simulating the stress strain history over a long time frame relevant for cap design or cap evaluation. A research centrifuge can be used to model prototype conditions and accelerate flow through porous media. The rationale behind centrifuge modeling is that the centrifugal acceleration induced at the end of a rotating beam may be used to model the earth's gravitational acceleration (g). On the geotechnical centrifuge, a small-scale model, built to a scale of $1/N$, subjected to a centrifugal acceleration $N \times g$, experiences a stress distribution identical to that in a full-scale prototype subjected to gravitational acceleration g on the Earth. In cases of flow through saturated porous media, the time for advection in the model varies inversely as the square of the acceleration scales, N [9]. For example, at $200 \times g$, a 1-day test using the centrifuge on a model that is 200 times smaller than the prototype represents 109-years of full-scale prototype behavior. Table 1 displays the scaling relationships for centrifuge experiments.

Numerous investigators have conducted centrifuge modeling of flow through porous media and consolidation of fine-grained soils [10–18]. Researchers have concluded that appropriate scaling laws could be used to model flow processes on a research centrifuge. Numerous researchers have also studied contaminant (i.e. radioactive and organic) transport on the research centrifuge and have verified the utilization of research centrifuge to model environmental contaminant flow problems [19–23].

3. Materials characterization

The Los Angeles Army Corp of Engineer District supplied sediment from Marina del Rey and capping material from Queens Gate for use in this study. Physical and geotechnical

Table 2
Physical characteristics of sediment and cap

Parameter	ASTM method	Sediment	Cap
Sand (%)	D-422	85.6	64
Fines (%)	D-422	14.4	36
Water content (%)	D-2216	25.3	38.4
Organic content (%)	D-2974	1.0	1.8
Density (pcf) g/cm^3	–	(83.97) 1.35	(82.99) 1.33
Specific gravity	D-845	2.75	2.81
Void ratio	–	1.04	1.11
Porosity	–	0.51	0.53
Soil classification	D-2487	Silty sand	Silty sand
Effective size, D_{10} (mm)		0.06	0.03
Mean particle diameter (mm)		0.3	0.3
Hydraulic conductivity (cm/s)		2×10^{-3}	4.2×10^{-3}

analysis results for the sediment and cap materials are summarized in Table 2. The sediment and capping material are classified as silty sands according to the ASTM. Grain size distributions for the sediment and capping materials are shown in Fig. 1. Laboratory consolidation tests were conducted on the materials in accordance with the Corp of Engineers procedure in EM 110-2-5027, Confined Disposal of Dredged Material, for the purpose of estimating long term volume changes for a confined aquatic disposal (CAD) pit. Fig. 2 shows the laboratory consolidation test results for the sediment and capping material. The laboratory consolidation tests illustrate that both the sediment and capping material have low compressibility.

Table 3 shows the chemical characterization of the sediment and capping material along with the chemical analysis methods and detection limits. The results indicate the presence of high concentrations of iron and total organic carbon in the sediment and cap materials.

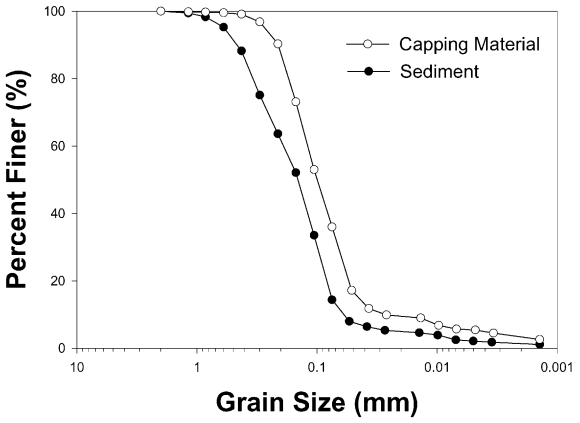

Fig. 1. Grain size distribution curve for sediment and cap.

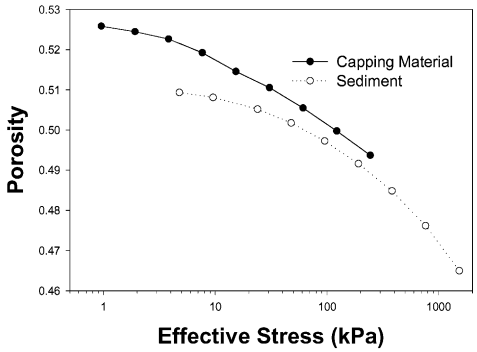

Fig. 2. Laboratory consolidation test results.

Furthermore, lead concentration in the sediment is higher than the lead concentration in the capping material. These results indicate that iron or lead may be transported from the sediment into the cap. However, due to radiochemical licensing requirement, it was not feasible to conduct testing on radiolabeled iron or lead. Thus, radiolabeled nickel chloride ($^{63}NiCl_2$) was chosen as a substitute.

Batch equilibrium tests following the procedure outlined by Roy et al. [24] were conducted on the capping material to determine the ability of the capping material to adsorb metals leached from the sediment. It was necessary to spike the sediment leachate with metals to increase the leachate contaminant levels to detectable limits and expose the capping material to a range of leachate metal concentrations. The spike solution, a mixed metal

Table 3
Chemical analysis of sediment and capping materials[a]

Parameter	Method[b]	Detection limits[c]			
		Water (mg/l)	Sediment (mg/kg)	Sediment (mg/kg)	Cap (mg/kg)
Arsenic	SW-846-7060	0.002	0.2	3.69	4.3
Cadmium	SW-846-7131	0.0005	0.2	0.39	0.14
Chromium	SW-846-6010	0.005	0.9	16.2	18.5
Copper	SW-846-6010	0.005	0.7	11.5	11.5
Iron	SW-846-6010	0.015	1.5	9490	12900
Lead	SW-846-7421 (water), SW-846-6010 (soil)	0.001	5	97.6	10.8
Mercury	SW-846-7470 (water), SW-846-7471 (soil)	0.0002	0.1	<0.04	<0.04
Nickel	SW-846-6010	0.007	10	10	9.2
Zinc	SW-846-6010	0.01	1.2	64.2	39.8
CEC	SW-846-9080	NA	NA	5.7	9.15
TOC	SW-846-9060	1	1	2680	2760
pH	SW-846-9045 (soil)	NA	NA	7.6	7.7

[a] NA: not applicable; CEC: cation exchange capacity; TOC: total organic carbon.
[b] US Environmental Protection Agency, 1997.
[c] Detection limits depend on sample size.

Table 4
Distribution coefficients (l/kg) for metals in capping material[a]

Compound	Percent metals sorbed by cap at a spiked concentration of				
	200 μg/l	300 μg/l	400 μg/l	500 μg/l	K_d
Arsenic	81.9	85.6	87.6	88.2	23
Mercury	99.9	99.9	99.9	99.9	7781
Nickel	97.1	97.0	96.0	97.8	67
Cadmium	99.5	99.8	99.6	99.9	4337[a]
Chromium	99.5	100	100	100	896[a]
Copper	99.0	99.3	98.5	99.2	441[a]
Lead	97.6	99.0	98.8	99.0	312[a]
Zinc	92.4	96.1	94.6	96.7	133[a]
^{63}Ni					339[b]

[a] Calculated from average of single point K_d's.
[b] Calculated from slope of the line (q vs. C).

standard (Supelco Inc., Bellefonte, PA) contained As, Cd, Cr, Cu, Pb, Hg, Ni, and Zn at concentrations of 1000 μg/ml. Batch equilibrium testing revealed that the capping material had a high affinity to sorb most of the metals tested. Evaluation of the batch equilibrium tests reveals that arsenic, mercury and nickel exhibited linear partitioning characteristics (Table 4). The remaining metals showed a more complex behavior, and the distribution coefficients were calculated by averaging the single point distribution coefficient determined for each spike concentration (Table 4) [25].

Nickel chloride ($^{63}NiCl_2$), a radiolabeled compound (denoted as ^{63}Ni) was used to study the transport of nickel through the cap material during the centrifuge tests. The ^{63}Ni isotope is a beta emitter that has a half-life of 100 years and emits 0.066 MeV. Radiolabeled nickel chloride was used in order to quantify nickel concentrations in thin sections (200 μm) of sediment and cap material and in small quantities of advected pore water. Quantification of unlabeled nickel in such thin sections is not possible due to the size of the analytical sample required.

Batch equilibrium tests were also conducted on the capping material to determine the sorption potential of radiolabeled ^{63}Ni. Fig. 3 shows the ^{63}Ni adsorption isotherm plot obtained from the batch equilibrium test for the capping material. The ^{63}Ni equilibrium distribution coefficient, K_d, for the capping material was 339 l/kg (slope of the isotherm) as shown in Table 4. The isotherm slope was obtained by linear regression using least squares analysis, and the coefficient of determination (r^2) was 0.99. It should be noted that the K_d value for ^{63}Ni was a factor of five higher than that obtained with unlabeled nickel (where $K_d = 67$ l/kg).

Rhodamine WT, a water-soluble, fluorescent dye was also used in this study to monitor the movement of pore water through the cap layer. Thirty kilograms of the sediment were weighed into an 8-gallon (0.03 m^3) stainless steel drum, and 120 ml of a 1 ppb solution of Rhodamine WT fluorescent dye solution were added to the sediment. The final concentration of dye in the sediment was 2000 μg dye per kilogram of sediment. The sediment was stirred on a mechanical mixer for at least 24 h. Dye was not added to the capping material.

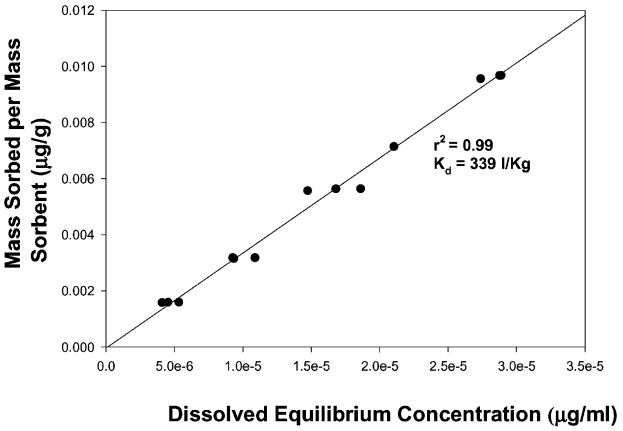

Fig. 3. Linear adsorption isotherm for ^{63}Ni with capping material.

4. Equipment

The research centrifuge has a radius of 6.5 m, and an acceleration range from $10 \times g$ to $350 \times g$. The maximum payload for the WES centrifuge is 8000 kg at an acceleration of $143 \times g$, and 2000 kg at an acceleration of $350 \times g$, see Fig. 4. Two modeling boxes were used in this study. To accommodate the instrumentation needed for consolidation measurements, a large diameter stainless steel (environmental) modeling box (with an inner diameter of 42 cm and height of 33 cm as shown in Fig. 5) was used to conduct the physical consolidation

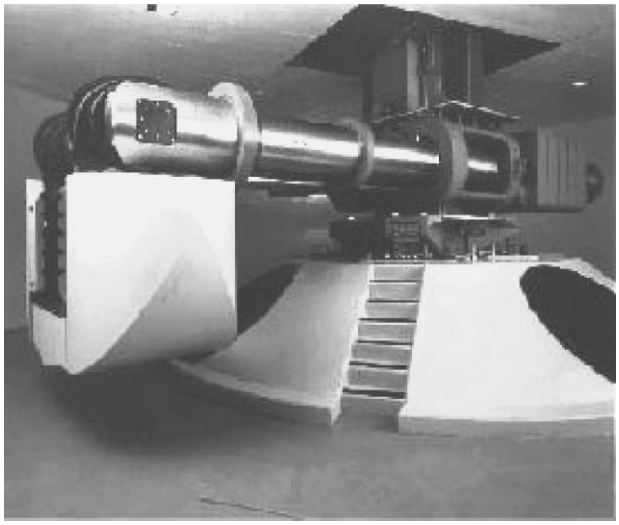

Fig. 4. WES centrifuge.

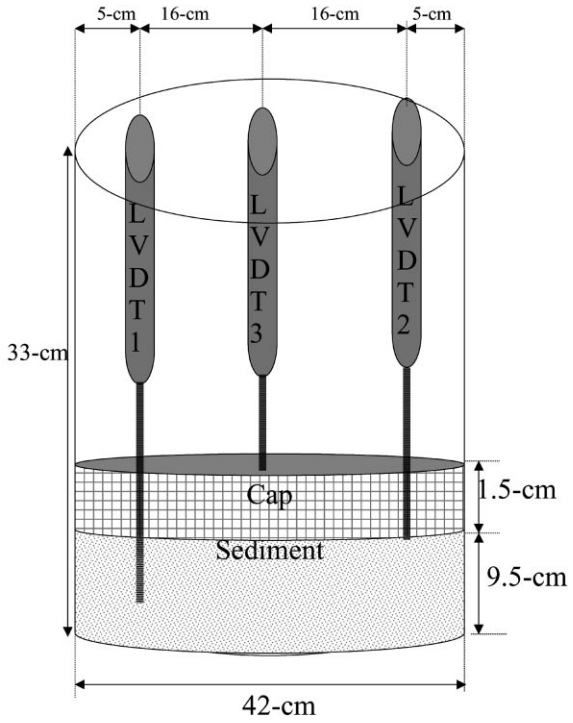

Fig. 5. Environmental modeling box with sediment, cap layer and LVDTs.

studies on the centrifuge. For the radiochemical tracer study, a smaller diameter modeling box fabricated from 1.75 cm thick, acrylic plastic with an inner diameter of 16.2 cm and a height of 25.4 cm was utilized. The smaller modeling box was used to reduce the quantity and cost of the radioisotope needed for the test and to adhere to site specific practices for conducting radiochemical tracer studies as a sealed source.

Linear variable differential transducers (LVDTs) were utilized in the centrifuge consolidation studies to measure the vertical settlement of the sediment. The LVDT is an electo-mechanical transducer that produces an electrical output proportional to the displacement of a separate movable core. A special footing was fabricated to allow the LVDT to remain on each surface layer before consolidation was induced. Each LVDT was mounted near the center of the modeling box with its foot placed on the surface of each layer of material.

Sediment samples were obtained from the modeling box using a 1.9 cm diameter plastic piston sampling devices. The sediment cores were then sectioned on a Carl Zeiss Inc., Model HM 440E microtome into thin sediment slices. The sediment slices were tested for water content, dye concentration, and for ^{63}Ni radioactivity. A Packard Bell TRI-CARB 2500 TR, multi-channel, liquid scintillation counter (LSC) was used for determining ^{63}Ni activity in the sediment slices and pore water samples. A Turner Model 10 Fluorometer was used to determine the dye concentration.

Table 5
Testing protocol for consolidation study

Procedure	Description	Test protocol
1	Bulk consolidation of dredged sediment	1. Add approximately 9.5 cm of the dye/sediment mixture to modeling box 2. Position an LVDT on the sediment surface, consolidate sediment on centrifuge for 4.375 min at 100 × *g* (1 month prototype) 3. Monitor surface settlement with LVDTs 4. Stop centrifuge, remove and weigh overlying fluid 5. Measure the magnitude of sediment settlement 6. Test dye concentration in overlying water
2	Cap sediment and centrifuge	1. Add 1.5 cm of capping material, measure heights 2. Position an LVDT on the surface of the capping layer 3. Centrifuge the sample for 7 h (eight prototype years) 4. Monitor surface settlement of cap and sediment with the LVDTs 5. Collect overlying water samples at 0.875, 3.25, 5.25, 7.02 h by stopping the centrifuge 6. Measure the height of the cap and sediment at the end of the consolidation test

5. Experimental procedures

Each centrifuge modeling box was coated with a thin layer of a high viscosity silicone oil (Dow Corning 510) in order to minimize side wall effects in the model and to prevent adhesion of the ^{63}Ni contaminant to the surface of the acrylic modeling box. The two sediment mixtures and the capping material were placed in separate large polyethylene bags. Loading of the modeling box to the desired sediment height and placement of the cap layer were accomplished by cutting open one corner of the polyethylene bags and slowly squeezing material out of the bag into the modeling box. After placement of the cap material, the cap was saturated with deionized water, and a 0.3 cm of overlying water was placed above the capping layer.

Table 5 lists the testing protocols for the centrifuge consolidation test, and Table 6 shows the protocols followed in conducting the radiochemical contaminant transport study. Overlying water samples were collected during the radioactive transport study at 1, 2, 4, 6, and 8 prototype years (0.875, 1.75, 3.5, 5.27, and 7.0 h during the test) to monitor concentration changes.

6. Experimental boundary conditions

The procedure outlined by Arulanandan et al. [14] was utilized to determine the flow regime where Darcy's law remained valid. For the limiting case when the Reynold's number is equal to one in the model, the maximum increase in the acceleration scale, $N_{\max}$, is given as follows:

$$N_{\max} = \frac{\nu n}{dk} i \tag{1}$$

Table 6
Testing protocol radiochemical advective transport test

Procedure	Description	Test protocol
1	Bulk consolidation of dredged sediment	1. Add approximately 9.5 cm premixed dye, radiolabeled ^{63}Ni and sediment mixture to modeling box 2. Consolidate on centrifuge for 4.375 min at 100 × g (1 month prototype time) 3. Stop centrifuge, remove and weigh overlying fluid 4. Measure magnitude of sediment settlement 5. Test dye and radiolabeled ^{63}Ni concentration in overlying water
2	Cap sediment and centrifuge for specified time	1. Add approximately 1.5 cm of capping material and record initial heights 2. Centrifuge the model for 7 h (eight prototype years) at 100 × g 3. Collect overlying water samples at 0.875, 1.75, 3.5, 5.25, and 7.02 h run time by stopping the centrifuge 4. Measure the height of the cap and sediment at the end of the test 5. Core sediment and cap model, test sediment cores for water content, radiolabeled ^{63}Ni and dye concentration

where ν is the kinematic viscosity, d the effective diameter, n the porosity, k the hydraulic conductivity, and i the hydraulic gradient. Assuming the hydraulic gradient is equal to 1 and the kinematic viscosity is equal to 10^{-6} m^2/s and using the hydraulic conductivity, porosity, and the effective particle size given in Table 2, Darcy's law remains valid as long as the acceleration scale is below 1500. Peclet number for these experiments is greater than one, which indicates that the hydrodynamic dispersion is a function of the velocity (note that the molecular diffusion for the capping material was 1.5×10^{-5} cm^2/s).

The centrifuge physical modeling study and radioactive transport tests were conducted at $100 \times g$, therefore, the centrifuge-model cap layer was 1.5 cm thick and the contaminated sediment layer was 9.5 cm thick. In conducting the centrifuge experiments, the contaminated sediment was consolidated for 0.0833 years (1 month) prototype time on the centrifuge prior to placing the cap layer. At $100 \times g$, 0.875 h in the centrifuge model is equal to approximately

Table 7
Boundary conditions for model and prototype

Boundary conditions	Test 1	Test 2
Centrifuge acceleration (g)	100	100
Model cap thickness (cm)	1.5	1.5
Prototype cap thickness (cm)	150	150
Initial water content cap (%)	38	38
Model sediment thickness (cm)	9.5	9.5
Prototype sediment thickness (cm)	950	950
Initial water content sediment (%)	41	41
Prototype area (m^2)	1385	248.3
Test duration (h)	7.08	7.08
Prototype time (years)	8.08	8.08

1 year of prototype time. To simulate 8 years in the prototype, centrifuge modeling was conducted for 7 h. Throughout the rest of this paper, the centrifuge data will be presented in prototype time. Table 7 summarizes the boundary conditions for the two centrifuge models.

7. Results and discussion

Centrifuge test 1 was conducted to determine the consolidation characteristics of the sediment and cap material. The environmental modeling box used in this test is shown in Fig. 5. Fig. 6 shows the centrifuge model and prototype settlement curve for test 1 after the placement of the cap. The total settlement in the model was 1.2 mm (i.e. 0.12 m in the prototype). In contrast to the LVDT results shown in Fig. 6, physical measurements from core samples indicated that approximately 0.5 cm (0.5 m in prototype) of total settlement occurred in the model. Due to the addition of water and dye solution to the sediment, the water content of the sediment mixture before consolidation was 41% which was higher than the initial sediment water content results shown in Table 2. During model preparation sediment was poured into the modeling box, therefore, the void ratio of the sediment mixture may have been higher than the initial sediment value reported (Table 2). The lack of sediment compaction prior to running the model may have contributed to the change in sediment settlement at the beginning of the test. Most of the settlement occurred within 1 month prototype time indicating immediate settlement as the primary mode of consolidation for the sediment. Fig. 7 shows the water content profile of the sediment and cap after completion of the test 1. The water content profile shows that the cap decreased in water content from 38% to an average of 26%, and the sediment mixture decreased in water content from 41% to an average of 23%.

Centrifuge test 2 was conducted to monitor the consolidation induced advective transport of ^{63}Ni. Because of safety concerns involved, centrifuge test 2 was conducted as a sealed source test with no instrumentation for measuring sediment settlement. Fig. 8 shows the

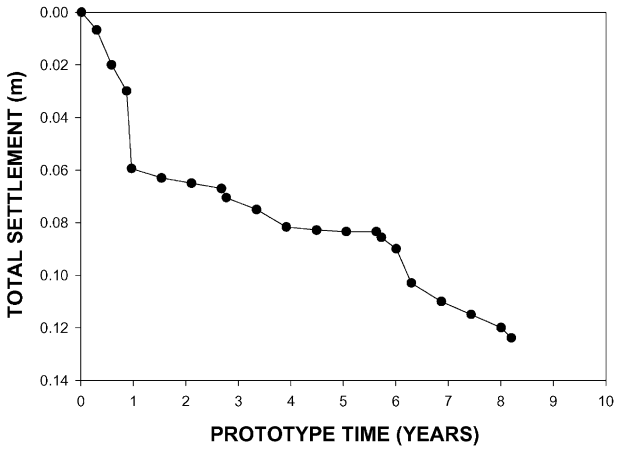

Fig. 6. Prototype settlement curve for centrifuge test 1.

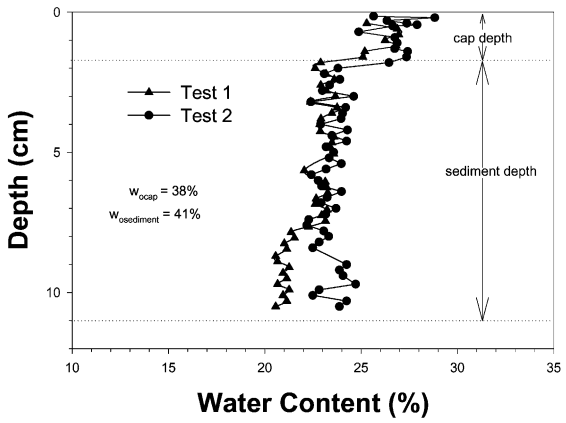

Fig. 7. Water content profile for the sediment and cap in centrifuge test 1.

Fig. 8. Acrylic modeling box with sediment and cap.

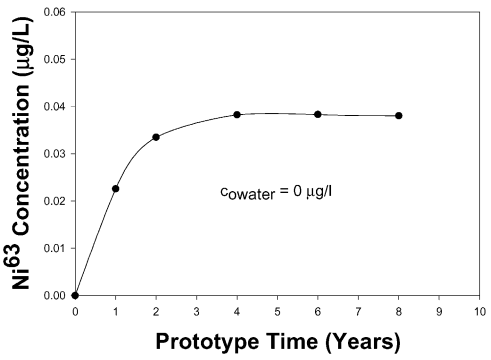

Fig. 9. Nickel concentration in overlying water in centrifuge test 2.

acrylic modeling box used in the test. Fig. 9 plots the ^{63}Ni concentration (in μg/l) versus the prototype time for the overlying water samples obtained during the centrifuge tests. Fig. 9 shows that the maximum concentration of ^{63}Ni advected from the sediment was 0.038 μg/l.

Fig. 10 shows the vertical profile of ^{63}Ni concentration for three sediment cores taken at the end of the test. In Fig. 10, the capping layers extend up to approximately 1.5 cm and the sediment layers ranges from ∼1.5 to ∼10.5 cm. An examination of the data in Fig. 10 illustrates that most of the ^{63}Ni remained in the sediment layer. This data indicate that minimal consolidation induced advective pore water transport of the ^{63}Ni occurred during the test. The distribution of ^{63}Ni in the sediment, cap layer and advected pore water at the end of eight prototype years is shown in Fig. 11. The data shows that the ^{63}Ni distribution in the sediment, cap, and overlying water are 99.5, 0.48 and 0.02%, respectively.

Fig. 12 shows the Rhodamine dye concentration versus prototype time for the overlying water samples obtained during the centrifuge test. This data shows an increase in dye concentration as time increases indicating that pore water moved from the sediment layer through the capping material. Fig. 13 illustrates a vertical profile of the Rhodamine dye concentration in three-sediment core sample obtained at the end of the test. The dye con-

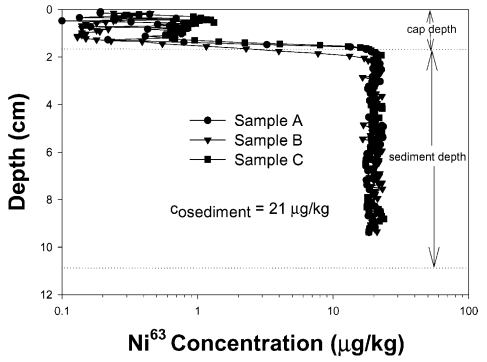

Fig. 10. The ^{63}Ni concentration in sediment and cap in centrifuge test 2.

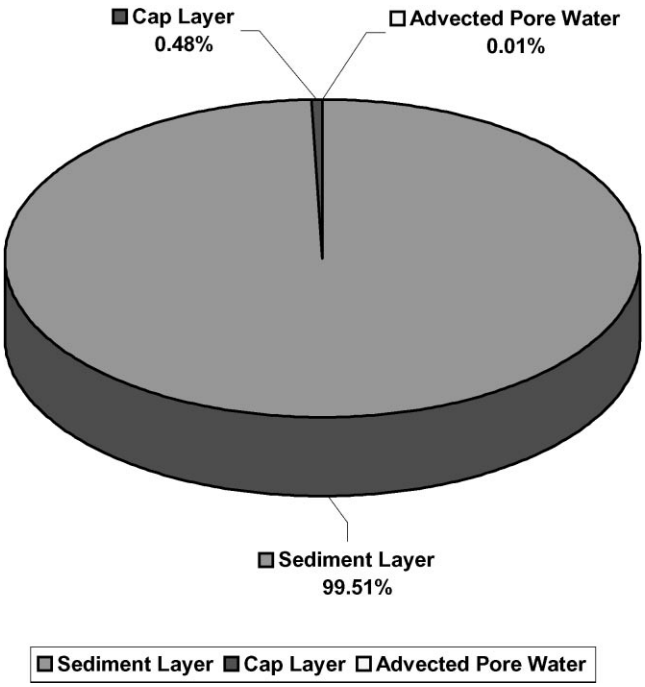

Fig. 11. The ^{63}Ni distribution after centrifuge test 2.

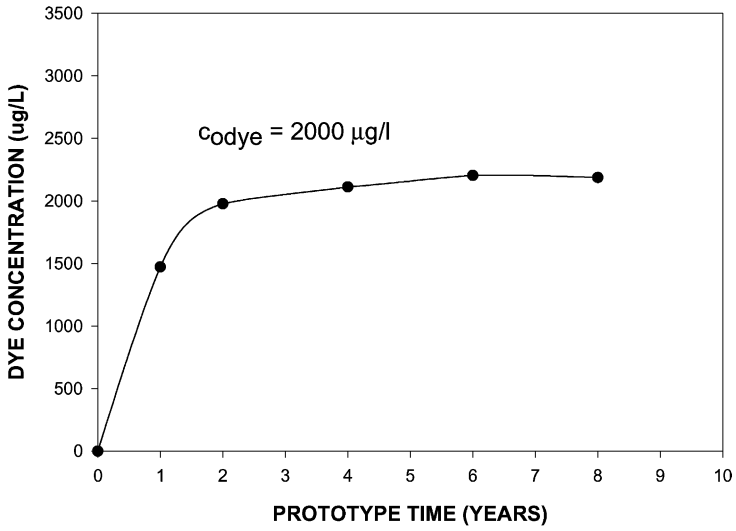

Fig. 12. Dye concentration in overlying water in centrifuge test 2.

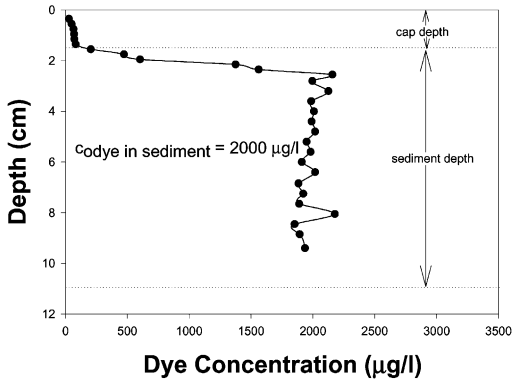

Fig. 13. Dye concentration in sediment and cap in centrifuge test 2.

centration in the advected pore water (Fig. 12) is similar to the dye concentration in the sediment (Fig. 13). The dye concentration is much greater in the sediment layer than in the cap layer indicating minimal adsorption of the dye by the capping material. Fig. 7 illustrates the water content profile for the sediment and cap at the end of test 2. The water content results for test 2 are similar to the results shown for Centrifuge Test 1. This indicates that pore water movement did occur during the centrifuge tests.

8. Mathematical modeling

Advection, hydrodynamic dispersion, and sorption govern the transport of metal contaminants through porous media. Advection is the transport of dissolved solutes by the movement of bulk fluids under a hydraulic gradient and is related to the seepage velocity. The seepage velocity is equal to the ratio of Darcy's velocity to porosity. Hydrodynamic dispersion is a function of molecular diffusion and mechanical dispersion. Molecular diffusion is the movement of dissolved molecular species from a region of high concentration to a region of low concentration. Mechanical dispersion is the dilution and spreading of a contaminant that results from the variation in the fluid velocity and the roughness and tortuosity of the pore channels. Sorption is the interphase transfer of dissolved contaminants from the aqueous phase to the solid phase. Sorption retards contaminants transport and can be equilibrium-controlled or rate-limited depending on the pore water velocity and chemical properties of the contaminant and solid phase. Sorption is the interphase transfer of dissolved contaminant from the aqueous phase to the solid phase [26].

van Genuchten and Alves [27] have provided a compendium of many analytical solutions to the advection–dispersion equation. The one-dimensional form of the advection–dispersion equation with linear equilibrium-controlled sorption and no reaction is as follows:

$$R_{\mathrm{f}}\frac{\partial c}{\partial t} = D_{\mathrm{A}}\frac{\partial^2 c}{\partial z^2} - v_{\mathrm{z}}\frac{\partial c}{\partial z} \tag{2}$$

where t is the time, v_z the seepage velocity, z the depth, R_f the retardation factor $= 1 + K_d\rho/n$, D_A the hydrodynamic dispersion coefficient, c the concentration, ρ the bulk density,

and n the porosity.

$$K_{\mathrm{d}} = \frac{S}{C} \tag{3}$$

where K_{d} is the partitioning coefficient (l/kg), S the contaminant concentration in the sediment at equilibrium (mg/kg), and C the contaminant concentration in the aqueous phase at equilibrium (mg/l).

In this portion of the study, advection–dispersion equation was used to estimate transport parameters of the centrifuge model. Moreover, in studying the transport of radioactive nickel through the cap, the semi-infinite region with uniform initial concentration with a constant flux boundary condition model was utilized. The initial and boundary conditions were as follows:

$$c(z,t)|_{t=0} = c_i, \quad z \in [0,0] \tag{4}$$

$$-D_{\mathrm{A}}\frac{\partial c}{\partial z}|_{z=0} + v_{\mathrm{z}}c(z,t)|_{z=0} = v_{\mathrm{z}}c_0, \quad t > 0 \tag{5}$$

$$\frac{\partial c}{\partial z}|_{z=0} = 0\,, \quad t > 0 \tag{6}$$

The solution to Eq. (1) with the initial and boundary conditions given above is as follows:

$$c(z,t) = c_i + (c_0 - c_i)\left[\frac{1}{2}\mathrm{erfc}\left(\frac{R_{\mathrm{f}}z - v_{\mathrm{z}}t}{2\sqrt{D_{\mathrm{A}}R_{\mathrm{f}}t}}\right) + \sqrt{\frac{v_{\mathrm{z}}^2 t}{\pi D_{\mathrm{A}}R_{\mathrm{f}}}}\exp\left(-\frac{(R_{\mathrm{f}}z - v_{\mathrm{z}}t)^2}{4D_{\mathrm{A}}R_{\mathrm{f}}t}\right) - \frac{1}{2}\left(1 + \frac{v_{\mathrm{z}}z}{D_{\mathrm{A}}} + \frac{v_{\mathrm{z}}^2 t}{D_{\mathrm{A}}R_{\mathrm{f}}}\right)\exp\left(\frac{v_{\mathrm{z}}z}{D_{\mathrm{A}}}\right)\mathrm{erfc}\left(\frac{R_{\mathrm{f}}z + v_{\mathrm{z}}t}{2\sqrt{D_{\mathrm{A}}R_{\mathrm{f}}t}}\right)\right] \tag{7}$$

In conducting this analysis, the sediment–water partitioning coefficient is defined by rearranging the terms in Eq. (1) with an initial concentration of ^{63}Ni in the sediment of 21 μg/kg. In modeling the advection–dispersion solution in Eq. (7) to the observed centrifuge data, three modeling scenarios are presented in this paper that are based on assumption made for the sediment–water partitioning coefficient, which is used to estimate the value of the dissolved ^{63}Ni in the sediment pore water:

1. No partitioning of the contaminant occurs in the sediment layer, where the pore water advected from the sediment into the capping layer will be equal to the initial contaminant concentration.
2. Contaminant partitioning occurs in the sediment layer and the partitioning coefficient of the sediment layer is approximately equal to the partitioning coefficient of the capping layer.
3. Contaminant partitioning occurs in the sediment layer and the partitioning coefficient of the sediment layer is approximately two times the partitioning coefficient of the capping layer.

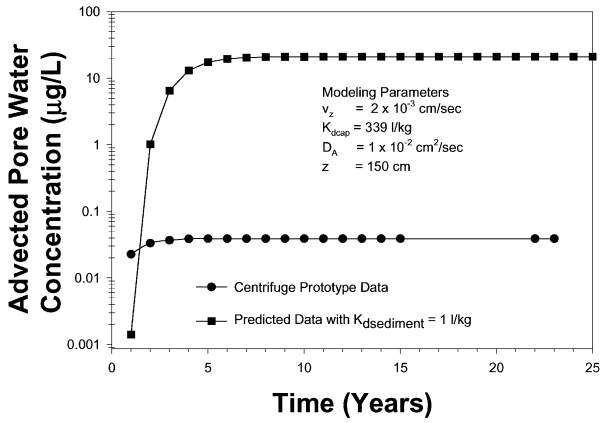

Fig. 14. Comparison of observed centrifuge data to advection–dispersion equation predictions for a sediment–water partitioning coefficient of 1.

The seepage velocity is estimated to be 2×10^{-3} cm/s from the hydraulic conductivity and the porosity provided in Table 2. To conduct this analysis, reasonable estimates for the hydrodynamic dispersion coefficient were utilized (i.e. ranging from 10^{-2} to 10^{-4} cm^2/s) [26].

The sediment–water partitioning coefficient varies with the contaminant and the characteristic of the soil system. For the first modeling scenario, the sediment–water partitioning coefficient was assumed to be 1 l/kg, which indicates that the initial concentration, c_0, of the pore water in the sediment is equal to the concentration in the soil of 21 μg/l. Fig. 14 shows the comparison of observed centrifuge data to advection–dispersion equation predictions for a sediment–water partitioning coefficient of 1 l/kg with an estimated hydrodynamic dispersion coefficient of 10^{-2} cm^2/s. It should be noted that as the hydrodynamic dispersion coefficient decreased, the time for breakthrough increased. Fig. 14 illustrates that the predicted maximum contaminant breakthrough (28.4 μg/l) is three orders of magnitude greater than the observed maximum contaminant breakthrough (3.38×10^{-3} μg/l) from the centrifuge results.

In the second modeling scenario, the sediment–water partitioning coefficient was assumed to be equal to the partitioning coefficient of the capping material. From Eq. (3), the concentration of the solute in the liquid phase of the sediment (i.e. initial concentration, c_0, in Eq. (7)) was assumed to be equal to 0.062 μg/l. Fig. 15 shows the comparison of the observed centrifuge data to advection–dispersion equation predictions with partitioning of the contaminant to the sediment equal to that of the partitioning coefficient of the cap. Fig. 15 illustrates that the predicted maximum contaminant breakthrough is greater than the observed maximum contaminant breakthrough in the centrifuge test by a factor of 2.

Fig. 15 also shows the third modeling condition, where the sediment–water partitioning coefficient is assumed to be equal to two times the partitioning coefficient of the capping material, and the initial concentration, c_0, in Eq. (7) is equal to 0.031 μg/l. The predicted concentration from the advection–dispersion equation follows a similar trend to the centrifuge

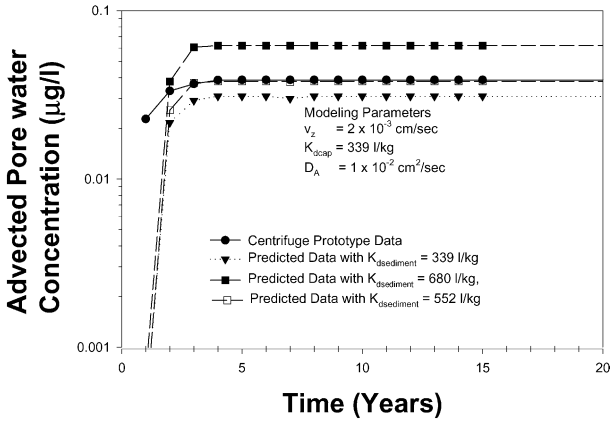

Fig. 15. Comparison of the observed centrifuge data to advection–dispersion equation predictions with partitioning of the contaminant to the sediment.

test. During the first 2 years, the advection–dispersion equation predicts a slightly lower concentration in comparison to the centrifuge data. The best advection–dispersion model prediction for the centrifuge data was obtained at a sediment water partitioning coefficient of 552 l/kg.

9. Synthesis

The dominant mechanism for this study was advection. For advective transport, the breakthrough time through the capping layer was predicted by utilizing the following equation:

$$t_b = \frac{LR_f}{v} \tag{8}$$

where L is the length of the capping layer [25]. The predicted breakthrough time for the capping layer was 2 years. The time for complete breakthrough in the centrifuge prototype is higher (4 years). This indicates that the transport phenomena in the centrifuge test were affected by hydrodynamic dispersion. This conclusion is also supported by the relationship between the ratio of the hydrodynamic dispersion to molecular diffusion and Peclet number, which illustrates that mechanical dispersion is the dominant transport process [13].

Arulanandan et al. [14] indicated that advective transport can be simulated even if the dispersion coefficient is violated. In addition, since the dispersion coefficient becomes larger in the model than in the prototype, the transport due to dispersion is faster in the model than it should be for similarity. This error is on the conservative side when considering the transport of pollutants. In this study, the centrifuge modeling results are considered to be conservative. In comparing the advection–dispersion equation to the centrifuge model, there were two unknown values: sediment to water distribution coefficient and the hydrodynamic dispersion coefficient. There were two trends in conducting the sensitivity analysis of the advection–dispersion equation for modeling the centrifuge results: as the sediment to water

distribution coefficient increased, the contaminant concentration into the overlying water decreased. As the hydrodynamic dispersion coefficient decreased, the time for the contaminant to breakthrough increased. In comparison to the test results conducted by Arulanandan et al., the predicted hydrodynamic dispersion coefficient from the advection–dispersion equation was one to two orders of a magnitude greater.

10. Conclusions

The objective of this research is to evaluate the significance of consolidation induced convective transport of radiolabeled inorganic contaminants from sediment into caps using a research centrifuge. Batch equilibrium tests were conducted to determine the adsorption potential of the capping material. The capping material has a high affinity to sorb heavy metal. The capping material exhibited a high sorption potential for radiolabeled nickel in comparison to nickel.

A centrifuge consolidation test was conducted to estimate the settlement of the sediment and cap. The sediment and cap were classified as silty sands, and exhibited low compressibility. A centrifuge test was conducted to determine the significance of consolidation induced convective transport of radiolabeled inorganic contaminants through a cap. Centrifuge test results illustrate that advection and dispersion were the dominant transport processes. The movement of water during the centrifuge test was illustrated by the transport of dye from the sediment through the cap and into the overlying water. Core samples taken at the end of the centrifuge test also showed the transport of ^{63}Ni and dye from the sediment and into the cap.

The centrifuge test result was compared to the advection–dispersion equation to predict contaminant transport parameters (i.e. sediment to water partitioning coefficient and hydrodynamic dispersion coefficient). The advection–dispersion equation demonstrated that the centrifuge test is a conservative estimate for predicting the transport of contaminants.

Acknowledgements

The work reported herein was conducted for the Headquarters, US Army Corp of Engineers (HQUSACE). The Army Corps of Engineers Los Angeles District provided funds for this work. The work was conducted under the direct supervision of Mr. Daniel E. Averett, Chief, ERB, Mr. Norman R. Francingues Jr., Acting Chief, EED; and under the general supervision of Dr. William F. Marcuson, Director, Geotechnical Laboratory, and Dr. John W. Keeley, Director, Environmental Laboratory. The authors would also like to thank Dr. Dean Adrian of Louisiana State University and Paul Schroeder of Waterways Experiment Station for their help in preparing this document.

References

[1] National Research Council. Contaminated Sediment in Ports and Waterways: Cleanup Strategies and Technologies, National Academy Press, Washington, DC, 1997, p. 295.

[2] US Army Corp of Engineers and US Environmental Protection Agency. Evaluating Environmental Effects of Dredging Material Management Alternatives — A Technical Framework. EPA 842-B-92-008, Washington, DC, 1992.
[3] T.H. Wakeman, P. Dunlop, L. Knutson. In: J.N. Meegoda, T.H. Wakeman, A. Arulmoli, W. Librizzi (Eds.), Dredging and Management of Dredged Material: Geotechnical Special Publication 65, American Society of Civil Engineers, Reston, 1997, pp. 12–22.
[4] M. Palermo, S. Maynord, J. Miller, D.D. Reible, Guidance for In-Situ Subaqueous Capping of Contaminated Sediment. EPA 905-B96-004, Great Lakes National Program Office, Chicago, IL, 1998.
[5] M. Palermo, J. Wilson, In: J.N. Meegoda, T.H. Wakeman, A. Arulmoli, W. Librizzi (Eds.), Dredging and Management of Dredged Material: Geotechnical Special Publication 65, American Society of Civil Engineers, Reston, 1997, pp. 1–11.
[6] X.Q. Wang, L.J. Thibodeaux, K.T. Valsaraj, D.D. Reible, Environ. Sci. Technol. 25 (9) (1991) 1578–1584.
[7] G.J. Thoma, D.D. Reible, K.T. Valsaraj, L.J. Thibodeaux, Environ. Sci. Technol. 27 (12) (1993) 2412–2419.
[8] D.M. DiTorro, J.S. Jeris, D. Ciarcia, Environ. Sci. Technol. 19 (12) (1985) 1169–1175.
[9] A. Lyndon, A.N. Schofield, Can. Geotech. J. 15 (1978) 1–13.
[10] D.J. Gooding, in: W.H. Craig (Ed.), Application of Centrifuge Modeling to Geotechnical Design, Balkema, Rotterdam, 1984, pp. 1–22.
[11] M. Muskat, The Flow of Homogeneous Fluid Through Porous Media, McGraw-Hill, New York, 1937.
[12] K.W. Cargill, H.Y. Ko, J. Geotech. Eng. 109 (4) (1983) 536–555.
[13] P. Croce, V. Pane, D. Znidarcic, H.Y. Ko., H.W. Olsen, R.L. Schiffman, in: W.H. Craig (Ed.), Application of Centrifuge Modeling to Geotechnical Design, Balkema, Rotterdam, 1984, p. 492.
[14] K. Arulanandan, P.Y. Thompson, B.L. Kutter, N.J. Meegoda, K.K. Muraleetharan, C. Yogachandran, J. Geotech. Eng. 144 (1988) 185–205.
[15] I. Ibrahim, Centrifugal modeling of water movement in unsaturated soils, Ph.D. Thesis, University of Colorado, Boulder, CO, 1990.
[16] G.F. Goforth, F.C. Townsend, D. Bloomquist, in: W.H. Craig, R.J. James, A.N. Schofield (Eds.), Centrifuge in Soil Mechanics, Balkema, Rotterdam, 1988, p. 274.
[17] D.J. Goodings, in: C.F. Leung, F.H. Lee, T.S. Tan (Eds.), Centrifuge 94, Balkema, Rotterdam, 1994, pp. 393–398.
[18] A.B. Cooke, R.J. Mitchell, in: H.Y. Ko, F.G. McLean (Eds.), Centrifuge 91, Balkema, Rotterdam, 1991, pp. 503–508.
[19] H.P. Villar, C.M. Merrifield, in: C.F. Leung, F.H. Lee, T.S. Tan (Eds.), Centrifuge 94, Balkema, Rotterdam, 1991, pp. 363–368.
[20] T.F. Zimmie, M.B. Mahmud, A. De, Can. Geotech. J. 31 (1994) 683–691.
[21] M.T. Chipley, Centrifuge modeling of flow processes, Ph.D. Thesis, University of Colorodo, Boulder, CO, 1996.
[22] R.J. Mitchell, Can. Geotech. J. 31 (1994) 357–363.
[23] J.A. Theriault, R.J. Mitchell, Can. Geotech. J. 34 (1997) 71–77.
[24] W.R. Roy, I.G. Krapac, S.F.J. Chou, R.A. Griffin, Batch-Type Procedures for Estimating Soil Adsorption of Chemicals, US Environmental Protection Agency Technical Resource Document, Washington, DC, Doc. No. EPA/530-SW-87-006-F, 1991.
[25] T.E. Myers, D.E. Averett, T.J. Olin, M.R. Palermo, D.D. Reible, J.L. Martin, S.C. McCutcheon, Estimating Contaminant Losses from Components of Remediation Alternatives for Contaminated Sediment. 905-R96-001, Great Lakes National Program Office, US Environmental Protection Agency, Chicago, IL, 1996.
[26] C.W. Fetter, Contaminant Hydrogeology, 2nd Edition, Prentice-Hall, Upper Saddle River, NJ.
[27] M.Th. van Genuchten, W.J. Alves, Analytical Solutions for the one dimensional convective–dispersion solute transport equation, Technical Bulletin No. 1661, US Department of Agriculture, 1982.